

# Evolution enhances the mutational robustness and suppresses emergence of a new phenotype

Tadamune Kaneko

*Department of Physics, Osaka University and  
Cybermedia Center, Osaka University*

Macoto Kikuchi\*

*Cybermedia Center, Osaka University  
Department of Physics, Osaka University and  
Graduate School of Frontier Bioscience, Osaka University*

Mutational robustness is an indispensable trait that living systems must possess. This property developed through a long history of evolution. In this paper, we discuss the evolutionary enhancement of mutational robustness for a toy model of the gene regulatory network (GRN). For exploring the particularity of evolution, we need a reference system. Such a reference system that we consider appropriate is a set of randomly sampled GRNs. However, since GRNs with high fitness are rare, a simple random sampling method is of no use for this purpose. Recently, Nagata and Kikuchi (PLoS Comput Biol 16 (2020) e1007969) proposed an efficient procedure for randomly sampling GRNs in a wide range of fitness based on the multicanonical Monte Carlo method. We employ that method to construct the reference set and compare it with the lineages obtained by evolutionary simulations. We consider a neural-network-like model of GRN, which has one input gene and one output gene. The fitness is defined so that it is large when the difference in the expressions of the output gene between two input values (“on” and “off”) becomes large. By comparing the evolution of fitness and the fitness distribution of the reference set, we find that evolution slows down significantly near the value of fitness that the number of GRNs becomes extremely rare. It implies that the evolutionary speed is determined mainly by the number of available GRNs, or in other words, “entropy”. Random sampling reveals that the highly-fit GRNs in this model inevitably exhibit bistability. Accordingly, the evolutionary simulations produce bistable GRNs as fitness becomes high. But the increase in the fraction of bistable GRNs occurs at higher fitness than the reference set. Thus, the emergence of a new phenotype, bistability, is delayed in evolution. We also study an indicator for mutational robustness. While in the early stage of evolution, it coincides with that of the reference set, in the late stage, it becomes significantly higher than that of the reference set. In short, evolution enhances mutational robustness. The reason is that GRNs with fewer lethal edges, that is, GRNs having fewer such regulatory interactions that the fitness drops largely when cut, are selected by evolution. We also find that local network motifs are relevant to function but irrelevant to mutational robustness. Thus mutational robustness is a property related to a global structure of GRNs. While those results are intuitively natural, we show them quantitatively by our method.

## I. INTRODUCTION

Living systems have developed their specific functions through a long history of evolution. Not only adaptation to the environment, but they have also acquired many kinds of robustness, such as the one against environmental noises as well as internal noises and the one against mutation of genomes.[1–3] Among them, the most important is the mutational robustness, by which a living system does not lose its function and can continue its life even when the genome is mutated.

Mutational robustness has been demonstrated experimentally. For example, comprehensive single-gene knock-out experiments for bacterium and yeasts have revealed that most of the knock-outs do not affect viability.[4–6] An artificial rewiring experiment for the gene regulatory network of *E. Coli* also has shown that the bacteria is

robust for most of the artificial additions of regulatory links.[7] Since living systems are subjected constantly to genetic mutations, if they easily lost their functions, such systems could not have produced offsprings during the evolutionary process. Thus, the mutational robustness must have also evolved through the evolutionary process along with the function. The central question we pose in this paper is whether the mutational robustness evolves.

However, as Wagner pointed out,[2] experimental studies on this issue would face difficulty more or less, because the existing living organisms are already the products of evolution, and evolutionary experiments can provide only outcomes reflecting the evolutionary pathways. Therefore, numerical methods play indispensable roles in obtaining information. In this study, we conducted a numerical investigation on the evolution of the mutational robustness using a toy model of the gene regulatory networks.

Genes coded on DNA in cells are read by RNA polymerase and transcribed to mRNA, whose information is then used to assemble proteins. A category of proteins

---

\* E-mail me at: kikuchi@cmc.osaka-u.ac.jp

called the transcription factors (TF) act as activators or repressors for other genes. Many genes regulate each other in this way and form a complex network called the gene regulatory network (GRN). GRNs are utilized to change the cell states to adapt to environmental change or to control the cell cycles or cell differentiation. One of the best known mathematical models of GRN is the boolean network model proposed by Kauffman, in which each fixed point of the dynamical system are considered to represent a cell state.[8–10].

To investigate whether the mutational robustness evolves or not, we need some reference system independent of evolutionary pathways. In the case of GRN, the reference system that we consider appropriate is the set of randomly-sampled GRNs. Random sampling is suitable to find universal properties that do not depend on histories of evolution. In this direction of research, Ciliberti *et al.* conducted a random sampling of GRNs to discuss mutational robustness.[11, 12] The fitness of their model was only two-valued: viable and non-viable. They investigated the interrelations of viable GRNs and argued that a majority of them belong to a large cluster connected by neutral mutations. However, such a simple random sampling method is not useful for systems having a more complex fitness landscape because highly-fit GRNs are very rare. Then, Burda *et al.* and Zagorski *et al.* employed the Markov-Chain Monte Carlo method to sample highly-fit GRNs.[13, 14] They found that GRNs exhibiting multi-stability contain some common network motifs. These researches focused on the universal properties of highly-fit GRNs.

The above methods are insufficient to sample GRNs in a wide range of fitness. Saito and Kikuchi proposed to utilize the Multicanonical Monte Carlo method (McMC) to investigate the mutational robustness of GRNs.[15] McMC has been developed originally in the field of statistical physics for sampling configurations within a wide range of energy evenly.[16, 17] But It has been realized to be useful also in sampling for nonphysical systems. It is particularly effective for generating very rare states and estimating the appearance probabilities of such rare states.[18–22]

By using McMC, Nagata and Kikuchi investigated a model of GRN.[23] They regarded fitness as the “energy” of GRNs and sampled GRNs randomly from very low fitness to very high fitness, and then classified them by fitness to explore their universal properties that are independent of the evolutionary pathway. Put concretely, they considered a neural-network-like model of GRN with one input gene and one output gene and set the fitness so that it is high if the GRN responded to change of input sensitively. Since each gene in their model did not respond ultrasensitively,[24, 25] and the network structures were restricted, simple network motifs did not give rise to bistability.[26] Despite that setting, they found that highly-fit GRNs always exhibited bistability. Thus, this bistability emerges as a consequence of the cooperation of many genes. According to their results, the new phe-

nototype that exhibits bistability appears whatever evolutionary path the system follows. In this case, the fitness function constrains the possible phenotype. Adding to that, they found that mutationally robust GRNs are not rare among such highly-fit GRNs. Thus the intuitive expectation that the optimization process would lead to mutational fragility is not necessarily correct for evolution of this model. Then, does evolution further enhance the mutational robustness?

To answer this question, we conducted evolutionary simulations. By comparing these results with the reference set of GRNs obtained by the method of Ref. [23], we discuss the universality and the characteristics of evolution.

## II. MODEL AND METHOD

To model GRN, we take into account only regulatory relations ignoring the details of gene expression. Such connectionist-type modeling has been used widely in theoretical studies.[23, 27–35] We represent a GRN as a directional graph by identifying nodes as genes and edges as regulatory interactions. We consider GRNs with one input node and one output node. In contrast to Ref. [23] that several restrictions were imposed to the network structure, we allow any network as long as the number of edges from one node to another is at most one. Thus, GRNs can contain auto-regulation and mutual regulation. Genes and edges that do not contribute to output are also permitted. As a result, the effective network size becomes smaller in general than the prepared size. In the following sections, we restrict ourselves to the networks of the number of nodes  $N = 32$  and the number of edges  $K = 80$ .

A variable  $x_i \in [0, 1]$  that represents the expression of a gene is assigned to each node with  $i$  the number of the gene.  $x_i$  obeys the following discrete-time dynamics: [28, 29]

$$x_i(t+1) = R \left( I\delta_{i,0} + \sum_j J_{ij}x_j(t) \right), \quad (1)$$

where  $t$  is the time step.  $J_{ij}$  represents the regulation from the  $j$ -th gene to the  $i$ -th gene. For simplicity, we assume that  $J_{ij}$  takes one of the three values,  $0, \pm 1$ ;  $+1$  indicates activation,  $-1$  indicates repression, and  $0$  means the absence of regulation. The  $0$ th gene is the input gene, and  $I \in [0, 1]$  is the strength of the input signal.[34] The response of the genes is given by the following sigmoidal function:

$$R(x) = \frac{1}{1 + e^{-\beta(x-\mu)}}, \quad (2)$$

where  $\beta$  represents the steepness of the function, and  $\mu$  is the threshold. This function is used widely in theoretical studies.[30, 34–37] In the present study, we set  $\mu = 0$  and

$\beta = 2$ . These parameters are the same as those used for the neural network model by Hopfield and Tank[38] and give a rather gradual increase to the response function, which reflect the stochastic nature of gene expression.[35] The response function  $R(x)$  is not ultrasensitive in the sense that a single gene with this response function has a single fixed point even when the auto-activation loop is attached. Therefore, for multistability to emerge, many genes are necessary to act cooperatively. Although the spontaneous expression  $R(0) = 0.5$  is rather large, we do not consider it causes any problem for the present purpose.

We define fitness for this model. Following Ref. [23], we set the fitness so that it becomes large when the difference in the expression of the output gene between  $I = 0$  and 1 (“off” and “on”) is large. Let  $\bar{x}_{out}(I)$  be the corresponding output to input value  $I$ .  $\bar{x}_{out}(I)$  is the fixed-point value of the output gene for fixed  $I$ ; as the initial condition, we set the expression of all genes as 0.5, the spontaneous expression. If  $x_{out}(t)$  behaves oscillatory in time instead of reaching the fixed point, we use the temporal average for  $\bar{x}_{out}(I)$ ; the system reaches a fixed point in most cases. The fitness  $f$  is defined as follows:

$$f = |\bar{x}_{out}(0) - \bar{x}_{out}(1)|. \quad (3)$$

The fitness takes values in  $[0, 1]$  by definition.

We studied this model using two different methods. One is random sampling using the multicanonical Monte Carlo method (more precisely, entropic sampling,[39] which is one of the variations of the MCMC). Details of the method are described in Ref. [23]. We divided fitness into 100 bins and determined the weight for each bin so that the GRNs appeared evenly using the Wang-Landau method.[40, 41] One update of MCMC consisted of the following successive two processes: Deleting a randomly selected edge and putting a new edge to an unlinked gene pair that is also chosen randomly. Whether accepting this change or not was decided by the Metropolis method. One Monte Carlo step (MCS) consisted of  $K$  such updates, and we recorded  $f$  at every MCS. We sampled GRNs at every 20 MCSs to reduce the correlation between the samples. We conducted ten independent runs each of which consisting of  $10^7$  MCSs. As a result, we obtained 50000 samples on average for each bin. Ideally, we can gather GRNs randomly within each bin. Although inter-sample correlations remain to some extent, we call this method “the random sampling” in this paper. The set of these randomly sampled GRNs provides the reference set.

Another method is the evolutionary simulation. As the initial population, we generated 1000 GRNs randomly. In one step of evolution, we selected the top 500 GRNs according to the order of fitness and made one copy for each; then, these copies were subjected to mutation. The mutation operation for each GRN was the same as the procedure in the MCMC; an edge was deleted randomly from the network, and then a new edge was added between a randomly selected unlinked gene pair. As these

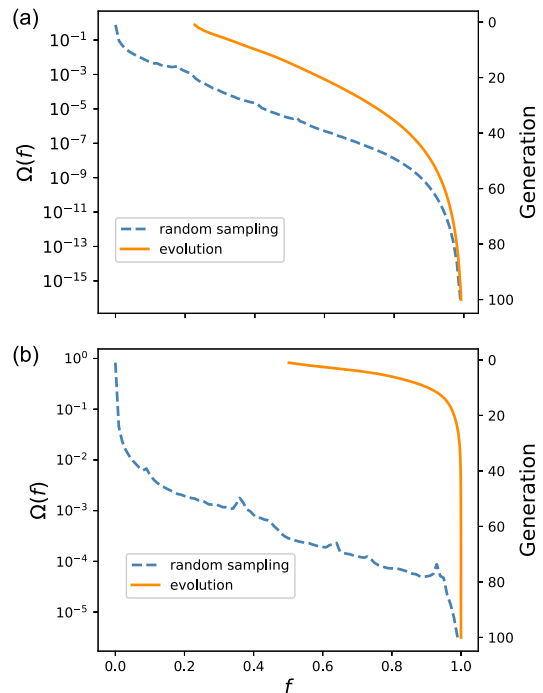


FIG. 1. Fitness landscape and evolution of fitness. Fitness  $f$  is divided into 100 bins. The blue dashed lines (left axis) show the appearance probability of each bin  $\Omega(f)$ , which was obtained by MCMC. The orange solid lines (right axis) is the average fitness of each generation by the evolutionary simulation. The averages are taken over 10000 lineages. (a)  $\beta = 2$  (b)  $\beta = 4$ .

procedures repeated, the average fitness of the population increased. After 150 generations, we picked the GRN having the highest fitness among the population and traced its ancestors to obtain a single lineage. The above population size and the number of generations were arbitrarily determined. We repeated this evolutionary simulation 10000 times independently, and as a result, we collected 10000 lineages.

### III. RESULTS

#### A. Fitness landscape and speed of evolution

The blue lines in Fig. 1(a) show the appearance probability  $\Omega(f)$  of each bin of fitness  $f$ . It can be called the fitness landscape. The sum of  $\Omega(f)$  is normalized to 1. The probability for  $f \geq 0.99$  is  $\sim 10^{-16}$ . Since we can count the total possible number of GRNs as  $\binom{N^2}{K} 2^K \simeq 10^{145}$ , the highly-fit GRNs are numerous but rare. Majority of GRNs concentrate near  $f \sim 0$ . GRNs decrease exponentially with  $f$ , and for very high  $f$ , they decrease faster than exponential. For comparison, we show the fitness landscape for steeper response function,  $\beta = 4$ , in Fig. 1(b). Although the fitness landscape is rough (This

roughness is not a statistical error), it is divided into three regions as in the case of  $\beta = 2$ .

The orange lines are the average fitness of each generation obtained by the evolutionary simulation. The vertical axis represents the generation in the downward direction. The evolution progresses almost linearly in the early stage and slows down drastically for large  $f$ . The values of  $f$  that the increase in fitness starts to slow down roughly coincide with the value that the faster-than-exponential decrease in  $\Omega(f)$  begins for both  $\beta = 2$  and 4. The reason is intuitively understandable: The number of the possible destination that a GRN can transit by the mutation is restricted by  $\Omega(f)$ . In other words, when the number of GRNs with higher fitness decreases drastically, the possibility that the fitness raises by chance also decreases. Since  $\log \Omega(f)$  can be called “entropy”, this result suggests that the evolutionary speed depends in large part on the entropy.

### B. Delayed emergence of bistability

The model in Ref. [23] exhibits bistability as  $f$  approaches its maximum value. Namely, the dynamical system reaches different fixed points for  $I = 0$  and 1. When  $I$  is changed continuously, two saddle-node bifurcations take place,[42] in contrast to the case of small  $f$  that a single fixed point moves to follow the change of  $I$ . We found that the present model behaves similarly.

The bistable GRNs are classified into three categories. The first is the toggle switch that two saddle-node bifurcations occur within  $I \in [0, 1]$ . The toggle switch is found, for instance, in phage  $\lambda$  and utilized for adaptation to environmental change.[43–46] The second is the one-way switch.[42] In this case, only one saddle-node bifurcation point is found in the range  $I \in [0, 1]$ , and another bifurcation point is out of this range. One-way switches give rise to cell maturation or cell differentiation; a typical example is the MAPK cascade in the maturation of the *Xenopus* oocyte.[47] In the last category, both of two bifurcation points are out of the range of  $I$ . Since this type may not work as a switch as long as the effect of noise is not taken into account, we call it “unswitchable”. In this paper, we do not distinguish these three and treat them equally as the bistable GRNs. It is straightforward to change the definition of bistability to deal only with, for example, toggle switches.

Fig.2 shows the fraction of the bistable GRNs  $P_2(f)$  against fitness. The blue line is the result of random sampling. The bistable GRNs starts to appear at  $f \simeq 0.5$  and increases rapidly until all the GRNs become bistable for  $f \rightarrow 1$ . Thus, the new phenotype that exhibits bistability emerges as the fitness increases, and all the GRNs converge to such a phenotype as the fitness approaches its maximum value. The orange line is  $P_2(f)$  obtained by evolutionary simulation. We classified GRNs in the obtained 10000 lineages by fitness as in the case of the random sampling. The figure clearly shows that  $P_2(f)$  of

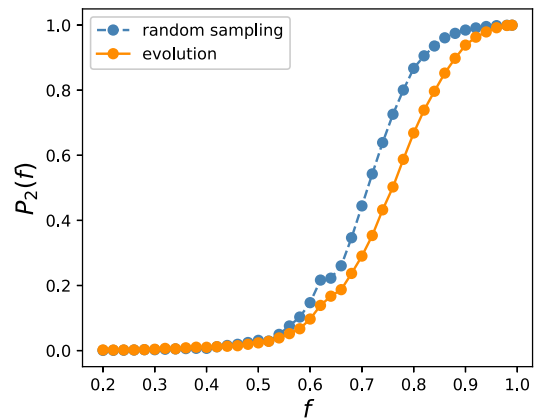


FIG. 2. Fitness dependence of the fraction of bistable GRNs. The orange solid line is for evolutionary simulation, and the blue dashed line is for random sampling. Bistability is checked as follows: First, starting from the steady-state at  $I = 0$ ,  $I$  was increased by 0.001, and the dynamics were run until the steady-state was reached. This procedure was repeated up to  $I = 1$ . Then, the inverse process from  $I = 1$  to 0 was performed. If the difference in  $\bar{x}_{out}$  larger than  $10^{-6}$  was observed between these two processes in some range of  $I$ , the GRN was regarded as bistable. GRNs obtained by evolutionary simulations were classified according to  $f$  into 100 bins similarly to random sampling.  $P_2(f)$  was calculated for every other bin.

the evolutionary simulation is significantly low compared to that of the random sampling at the same  $f$ . In other words, evolution delays the rapid increase of  $P_2(f)$ . It suggests that evolution tends to suppress the emergence of a new phenotype. The reason is that a lineage reflects its evolutionary history; nonetheless, the eventual emergence of the bistable phenotype is inevitable as the fitness increases because all the GRNs are bistable for  $f \rightarrow 1$ .

### C. Evolution of mutational robustness

To discuss mutational robustness, we introduce a measure for robustness. In Ref. [23], the single-edge deletion is considered as a mutation; it was found that the edges split into two classes, neutral and lethal, for highly-fit GRNs, and the lethal edges are minor among them. We consider the single-edge deletion as the mutation also for the present model and obtained the same results. Then, we defined the following quantity  $r$  as the robustness measure:

$$r \equiv \frac{1}{K} \sum_{i=1}^K f'_i, \quad (4)$$

where  $f'_i$  is fitness after the  $i$ th edge is deleted, and the sum is taken for all the edges. Since  $f'$  should have a tendency to increase with  $f$ , comparing  $r$  of GRNs with different  $f$  is not meaningful. However, by comparing

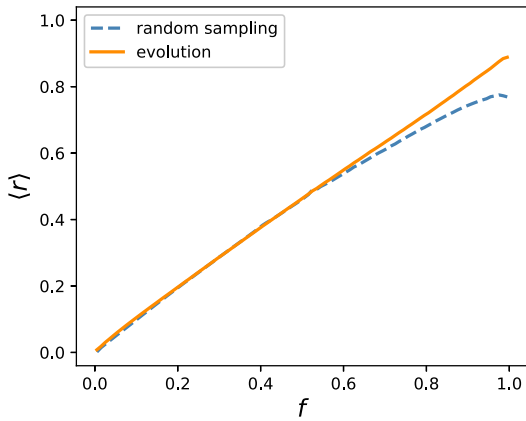


FIG. 3. Average of the robustness measure  $r$  against fitness. The average was taken over all the samples in each bin. The orange solid line is for evolutionary simulation, and the blue dashed line is for random sampling. The averages for evolutionary simulation were calculated by the reweighting method described in the text.

this quantity for GRNs obtained by random sampling and evolutionary simulation at the same  $f$ , we can discuss the particularity of evolution.

Fig3 shows the average of  $r$  against  $f$ . The average was taken over all the GRNs in the corresponding bin.  $\langle r \rangle$  obtained by evolutionary simulation increases monotonously and coincides with that obtained by random sampling up to  $f \simeq 0.5$ . For larger  $f$ , The value of evolution departs upward from that of random sampling, and the difference becomes more and more significant as  $f$  increases.

To scrutinize the difference, we show the probability distribution of  $f'$  for  $f = 0.5, 0.8$ , and  $0.99$  in Figs. 4(a)-(c), respectively. Here, the value of  $f$  indicates the lower bound of the bin; for example,  $f = 0.99$  means  $f \in [0.99, 1.0]$ . Taking into account that the distribution of  $f$  in each bin differs for random sampling and evolution, we divided each bin into ten sub-bins and reweighed the distribution obtained by evolutions so that the distribution of  $f$  coincides with that of random sampling (The values plotted in Fig.3 shown before were also calculated based on this reweighting method). We divided  $f'$  into 80 bins because otherwise, unnecessary oscillation appears in the distribution due to the discreteness of the number of lethal edges. While both distributions roughly agree for  $f = 0.5$ , we can see deviation for  $f = 0.8$ . The two distributions exhibit distinct difference for  $f = 0.99$ ; the distribution obtained by evolution is biased to large  $r$  compared to random sampling. Therefore, evolution enhances mutational robustness.

What causes this difference? As was stated before, the edges of randomly sampled GRNs for  $f \geq 0.99$  split into neutral and lethal. Namely, when we cut one edge,  $f'$  is either close to  $f$  or almost 0, and other types of edges are scarce. Based on this observation, we investigated the

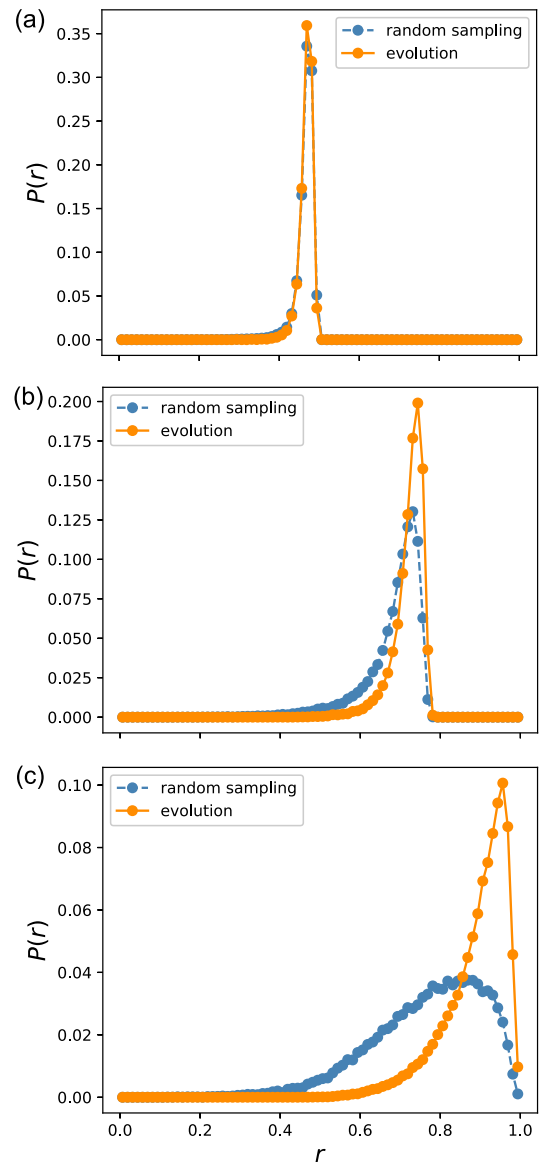


FIG. 4. Probability distribution of the robustness measure  $r$ . The orange solid line is for evolutionary simulation, and the blue dashed line is for random sampling. The distribution for evolutionary simulation were corrected by the reweighting method described in the text. (a)  $f \in [0.5, 0.51]$  (b)  $f \in [0.8, 0.81]$  (c)  $f \in [0.99, 1.0]$

number distribution of the lethal edges by defining that an edge is lethal if  $f' < 0.8$ . Although this definition is arbitrary, it hardly affects the result. Fig.5 shows the probability distribution of the number of the lethal edges  $n_L$  for  $f \geq 0.99$ . GRNs obtained by evolutionary simulation are biased significantly to the small number side compared to random sampling. The highest probability is at  $n_L = 3$ , and the distribution is narrow; moreover, more than 2% of GRNs have no lethal edge. In contrast, the highest probability for random sampling is at  $n_L = 15$ , and the distribution is much wider; GRNs lack-

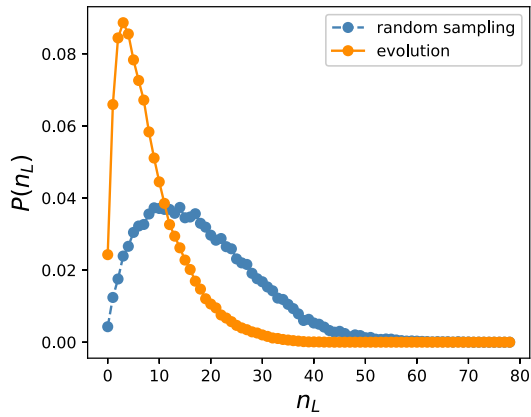


FIG. 5. Probability distribution of the number of lethal edges  $n_L$  for  $f \in [0.99, 1.0]$ . The orange solid line is for evolutionary simulation, and the blue dashed line is for random sampling. An edge is regarded as lethal if fitness after that edge is cut is less than 0.8. The distribution for evolutionary simulation were corrected by the reweighting method described in the text.

ing lethal edge are only 0.4%. Thus, it is clear that the smallness of the number of lethal edges is the reason for the enhancement of mutational robustness by evolution.

One possibility is that the nodes that affect the output are fewer in the evolutionary obtained GRNs. To check this, we counted the number of nodes  $n_N$  that have at least one path to the output node. Fig.6 shows the distributions; that for the random networks is also plotted for comparison. While the peak of the distribution is at  $n_N = 28$ , which is slightly fewer than the random networks, the distributions are indistinguishable between evolution and random sampling. Therefore, the number of effective nodes is not the reason for the difference in the number of lethal edges.

#### D. Motif analysis

Next, we investigate network motifs. In the model of Ref. [23], the coherent feedforward loops and the positive feedback loops were significantly abundant in highly-fit GRNs. Since the present model allows auto- and mutual-regulations, we also explored other patterns adding to the triangular patterns. Put concretely, we counted the number of auto-regulations, mutual-regulations between gene pairs, triangles, and mutual activation or repression of two nodes combined with auto-activation of both nodes. The last pattern frequently appears in multistable GRNs.[13, 43, 44, 48–50] Since the motifs are defined as the network patterns that are abundant compared to the random networks,[26, 51] we also counted them for the random networks.

As a result, the following patterns are more in number than the random networks: auto-activation, mutual-activation, mutual-repression, coherent feedfor-

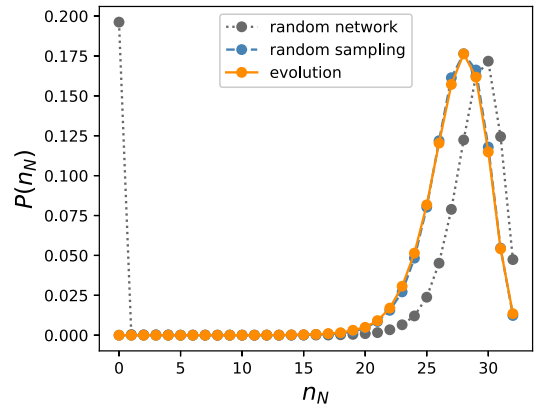


FIG. 6. Distribution of effective node number  $n_N$  for  $f \in [0.99, 1.0]$ . If a node has at least one path to the output node, that node is regarded as “effective”. The orange solid line is for evolutionary simulation, and the blue dashed line is for random sampling. The distribution for the random networks is also shown as a reference by the gray dotted line. The distribution for evolutionary simulation were corrected by the reweighting method described in the text.

ward loops (FFL+), positive feedback loops (FBL+), and mutual activation or repression plus auto-activation of two genes. We show their number distributions in Fig.7(a)-(f). Although their abundances are not so remarkable, we may call them motifs. Other patterns such as auto-repression, incoherent feedforward loop, and negative feedback loop are less than the random networks. The notable point here is that the distributions of these motifs are almost the same for both evolution and random sampling. Thus, whether or not these highly-fit GRNs are products of evolution is not reflected in distribution of these local motifs. Therefore, the difference between evolution and random sampling should lie in global network structures.

#### E. Path distribution

As a characteristic of the global structure, we counted the number of paths  $n_{path}$  connecting the input and the output. Fig. 8 shows the distribution of paths starting from the input node and reaching the output node without passing the same node twice. Two distributions exhibit a distinct difference; while the probability of GRNs with only one path reaches 4% for random sampling, it is 0.1% for evolution, and evolutionary obtained GRNs with the number of paths less than about 100 are fewer than those of random sampling. It suggests that the global structures of GRNs obtained by these two methods differ significantly. However, the difference in the path distribution does not explain all. Fig. 9 is a scatter plot of the number of paths and the number of the lethal edges. We took data for  $f \in [0.99, 0.991]$  from the evolutionary obtained GRNs. The figure clearly shows that the num-

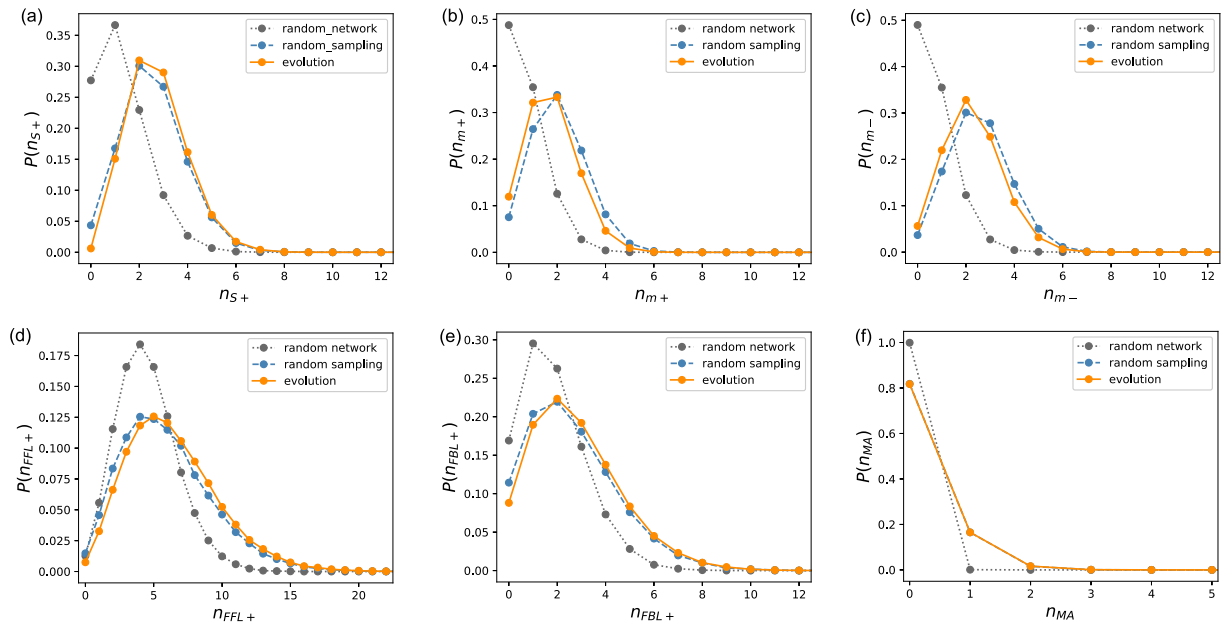


FIG. 7. Probability distributions of the number of motifs for  $f \in [0.99, 1.0]$ . The orange solid lines are for evolutionary simulation, and the blue dashed lines are for random sampling. The distributions for the random networks are also shown as references by the gray dotted lines. The distributions for evolutionary simulation were corrected by the reweighting method described in the text. (a) auto-activation (b) mutual activation (c) mutual repression (d) coherent feed-forward loop (e) positive feedback loop (f) mutual activation or mutual repression accompanied by auto-activation of both genes

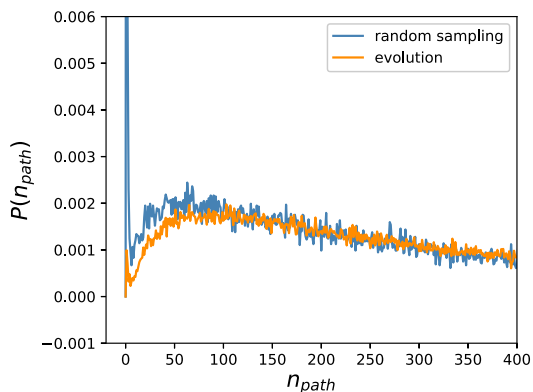


FIG. 8. Probability distribution of the number of paths  $n_{path}$  starting from the input node and reaching the output node without passing the same node twice.  $n_{path} \leq 400$  is shown. The orange line is for evolutionary simulation, and the blue line is for random sampling. For random sampling,  $P(1)$  reaches 4%.

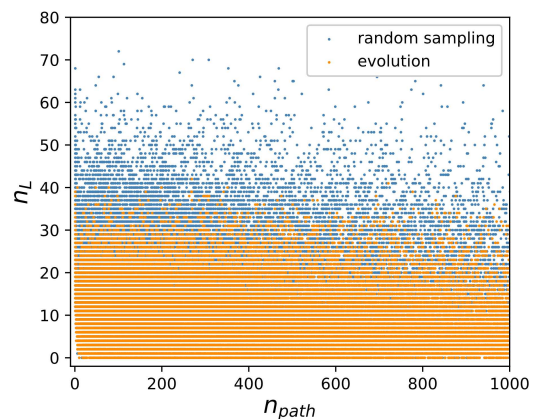


FIG. 9. Scatter plot of the number of paths  $n_{path}$  and the number of the lethal edges  $n_L$ .  $n_{path} \leq 1000$  is shown. The orange dots are for evolutionary simulation, and the blue dots are for random sampling. While the data for  $f \in [0.99, 1.0]$  are shown for random sampling, the data for  $f \in [0.99, 0.991]$  are shown for the evolutionary simulations.

ber of the lethal edges is less for evolution irrespective of the number of paths. It should be noted that even for  $n_{path} = 1$ , the number of the lethal edge distributes broadly. It means that the locations of the lethal edges are not limited to the “on-path” between the input node and the output node.

#### IV. SUMMARY AND DISCUSSIONS

We studied a toy model of gene regulatory networks and showed that evolution enhances mutational robustness and delays the emergence of a new phenotype. Both consequences are intuitively natural, and we were able to show them quantitatively by comparing the evolutionary

simulation with randomly sampled GRNs as a reference set. The multicanonical ensemble Monte Carlo method was effective in realizing random sampling of GRNs in the whole range of fitness.

The answer to the central question of this study, “does the mutational robustness evolve?”, is “yes”. In our model, evolution progresses in two stages; in the early stage, the measure of mutational robustness took the same values as random sampling. At the later stage, in contrast, mutational robustness is markedly enhanced as the fitness increases, compared to the randomly sampled set.

The mechanism for the enhancement of mutational robustness is intuitively understandable. The mutation we considered consists of two successive procedures: First, an edge selected randomly is deleted. Next, a new edge is added between a randomly selected node pair. As was shown in Ref. [23], the edges start to be divided roughly into two types at an intermediate value of fitness: neutral ones and ones that the fitness decreases substantially when deleted. Here we call the latter type “lethal”, although fitness does not necessarily drop close to zero unless fitness before the cut is large enough. If the deleted edge is lethal, fitness drops largely, and the possibility for fitness to recover by a randomly added new edge is very low. Therefore, the more lethal edges a GRN has, the harder its copy survives. In contrast, when a neutral edge is deleted, whether or not fitness increases is determined randomly. In this scenario, the mutational robustness evolves because GRNs containing many lethal edges are eliminated easily from the population. This mechanism is called “the second-order selection” according to Wagner.[2] Details of the selection process require further investigation.

The new phenotype, namely the GRNs exhibiting bistability, inevitably emerge as fitness increases. It is an example that fitness constrains phenotypes. We showed that even under such a situation, evolution behaves conservatively; the appearance of bistability is delayed significantly compared to random sampling. In other words, evolution proceeds so as not to allow easily the change in phenotype. As a result, the phenotypic change occurs rapidly at the last stage of evolution. This phenomenon may explain the punctuated equilibrium.

The emergence of the cooperative response of GRNs consisting of many genes having non-cooperative response function has been pointed out based on a numerical study.[35] Our result is consistent with that finding. From the experimental side, an example has been reported that a motif with non-cooperative response gives rise to the cooperative bistability when built in a larger GRN, although the mechanism of cooperativity is different from the present case.[59] In contrast, when the response of each gene is ultrasensitive, small motifs can be enough to exhibit bistability. The global structure of the network is expected to be different largely in such cases, and thus we consider that the present results apply mainly to large GRNs.

Next, we discuss network motifs. Some characteristic motifs are found for highly-fit GRNs, although not prominent compared to the model in Ref [23]; the reason for this difference is attributed to the difference in the allowed network structure. Among these motifs, coherent feedforward loops are a frequently observed motif in real GRNs.[26, 51, 52] The following structures are also identified as motifs, which are known to exhibit bistability if the response of each gene is ultrasensitive: [25, 47, 53–58] Auto-activation, mutual activation, mutual repression, and mutual activation/repression along with auto-activation. The last one is observed widely in multistable GRNs.[13, 43, 44, 48–50] Since the response function in our model is not ultrasensitive, the bistability is realized as a cooperative phenomenon of many genes. Nevertheless, these motifs are observed in our model, though not indispensable. They, however, are not relevant to mutational robustness. It implies that mutational robustness is related to the global structures of GRNs. We found that the number of paths connecting the input node and the output node differs between randomly sampled GRNs and evolutionary obtained ones. Although it is intuitively understandable that GRNs having many such paths are robust because of redundancy, this picture does not explain the origin of mutational robustness fully.

Evolutionary speed is roughly determined by the number of available GRNs or, in other words, “entropy”. It certainly is a consequence of the fact that we defined a single-valued fitness function, which can be computed from the dynamics of a given GRN for a predetermined single task and has the maximum value. This setup is somewhat artificial, and fitness is not such a simple function in reality. However, some evolutionary experiments correspond to the situation discussed in this paper. For example, Sato *et al.* reported such an experimental study.[60] They put DNA coding the green fluorescent protein (GFP) along with a random sequence to the genome of *E.Coli* and conducted an artificial evolution with the selection according to the fluorescence intensity. In this experiment, an observable single-valued fitness was set, which certainly has the maximum value. They found that the evolution speed slows down as the fluorescence intensity increases. It implies a decrease in the available genotype as fitness increases. They discussed that phenotypic divergence is relevant to evolutionary speed. Although we consider that the variation of evolutionary speed in their experiment is explained almost fully by the entropic effect, the relationship between phenotypic divergence and genotypic entropy requires further exploration. In the natural situation departed from the experimental condition, evolution is not restricted to proceed in one direction; when evolution to one direction becomes difficult, it will change direction. We consider that the concept of entropic effect on evolutionary speed can apply also to such a natural situation.

Finally, we should be careful about the model dependence. We believe that the three main results, that is, the evolution of mutational robustness, delay in the emer-

gence of a new phenotype, and relationship between evolutionary speed and genetic entropy, apply universally to other systems. Similar studies for different models and other objects are necessary to confirm.

## ACKNOWLEDGMENTS

The authors thank Koich Fujimoto, Katsuyoshi Matsushita, and Hajime Yoshino for fruitful discussions and comments.

- 
- [1] H. Kitano, *Nat Rev Genet* **5**, 828 (2004).
- [2] A. Wagner, *Robustness and Evolvability in Living Systems* (Princeton Univ Press, 2005).
- [3] J. Masel and M. L. Siegal, *Trends Genet* **25**, 395 (2009).
- [4] G. Giaever, A. M. Chu, L. Ni, C. Connelly, L. Riles, S. Veronneau, S. Dow, A. Lucau-Danila, K. Anderson, B. Andre, A. P. Arkin, A. Astromoff, M. E. Bakkoury, R. Bangham, R. Benito, S. Brachat, S. Campanaro, M. Curtiss, K. Davis, A. Deutschbauer, K. D. Entian, P. Flaherty, F. Foury, D. J. Garfinkel, M. Gerstein, D. Gotte, U. Gludener, J. H. Hegemann, S. Hempel, Z. Herman, D. F. Jaramillo, D. E. Kelly, S. L. Kelly, P. Kotter, D. LaBonte, D. C. Lamb, N. Lan, H. Liang, H. Liao, L. Liu, C. Luo, M. Lussier, R. Mao, P. Menard, S. L. Ooi, J. L. Revuelta, C. J. Roberts, M. Rose, P. Ross-Macdonald, B. Scherens, G. Schimmack, B. Shafer, D. D. Shoemaker, S. Sookhai-Mahadeo, R. K. Storms, J. N. Strathern, G. Valle1, M. Voet, G. Volckaert, C. Y. Wang, T. R. Ward, J. Wilhelmy, E. A. Winzeler, Y. Yang, G. Yen, E. Youngman, K. Yu, H. Bussey, J. D. Boeke, M. Snyder, P. Philippsen, R. W. Davis, and M. Johnston, *Nature* **418**, 387 (2002).
- [5] T. Baba, T. Ara, M. Hasegawa, Y. Takai, Y. Okumura, M. Baba, K. A. Datsenko, M. Tomita, B. L. Wanner, and H. Mori, *Mol Syst Biol* **2**, 2006.0008 (2006).
- [6] D. U. Kim, J. Hayles, D. Kim, V. Wood, H. O. Park, M. Won, H. S. Yoo, T. Duhig, M. Nam, G. Palmer, S. Han, L. Jeffery, S. T. Baek, H. Lee, Y. S. Shim, M. Lee, L. K. and K. S. Heo, E. J. Noh, A. R. Lee, Y. J. Jang, K. S. Chung, S. J. Choi, J. Y. Park, Y. Park, H. M. Kim, S. K. Park, H. J. Park, E. J. Kang, H. B. Kim, H. S. Kang, H. M. Park, K. Kim, K. Song, K. B. Song, P. Nurse, and K. L. Hoe, *Nat Biotechnol* **28**, 617 (2010).
- [7] M. Isaran, C. Lemerle, K. Michalodimitrakis, C. Horn, P. Beltrao, E. Raineri, M. Garriga-Canut, and L. Serrano, *Nature* **452**, 840 (2008).
- [8] S. A. Kauffman, *J Theor Biol* **22**, 437 (1969).
- [9] S. A. Kauffman and S. Levin, *J Theor Biol* **128**, 11 (1987).
- [10] S. A. Kauffman, *The Origins of Order: Self-Organization and Selection in Evolution* (Oxford Univ Press, 1993).
- [11] S. Ciliberti, O. C. Martin, and A. Wagner, *PLoS Comput Biol* **3**, e15 (2007).
- [12] S. Ciliberti, O. C. Martin, and A. Wagner, *Proc Natl Acad Sci USA* **104**, 13591 (2007).
- [13] Z. Burda, A. Krzywicki, O. C. Martin, and M. Zagorski, *Proc Natl Acad Sci USA* **108**, 17263 (2011).
- [14] M. Zagorski, A. Krzywicki, and O. C. Martin, *Phys Rev E* **87**, 012727 (2013).
- [15] N. Saito and M. Kikuchi, *New J Phys* **15**, 053037 (2013).
- [16] B. A. Berg and T. Neuhaus, *Phys Lett* **B267**, 249– (1991).
- [17] B. A. Berg and T. Neuhaus, *Phys Rev Lett* **68**, 9 (1992).
- [18] N. Saito, Y. Iba, and K. Hukushima, *Phys Rev E* **82**, 031142 (2010).
- [19] N. Saito and Y. Iba, *Comput Phys Commun* **182**, 223–225 (2011).
- [20] A. Kitajima and Y. Iba, *Comput Phys Commun* **182**, 251 (2011).
- [21] Y. Iba, N. Saito, and A. Kitajima, *Ann Inst Stat Math* **66**, 611 (2014).
- [22] A. Kitajima and M. Kikuchi, *PLoS ONE* **10**, e0125062 (2015).
- [23] S. Nagata and M. Kikuchi, *PLoS Comput Biol* **16**, e1007969 (2020).
- [24] A. Goldbeter and D. E. Koshland, *Proc Natl Acad Sci USA* **78**, 6840 (1981).
- [25] J. E. Ferrell and S. H. Ha, *Trends Biochem Sci* **39**, 496 (2014).
- [26] U. Alon, *An Introduction to Systems Biology (second edition)* (CRC Press, 2020).
- [27] E. Mjolsness, D. H. Sharp, and J. Reinitz, *J Theor Biol* **152**, 429 (1991).
- [28] A. Wagner, *Proc Natl Acad Sci USA* **91**, 4387 (1994).
- [29] A. Wagner, *Evolution* **50**, 1008 (1996).
- [30] M. L. Siegal and A. Bergman, *Proc Natl Acad Sci USA* **99**, 10528 (2002).
- [31] J. Masel, *J Evol Biol* **17**, 1106 (2004).
- [32] K. Kaneko, *PLoS one* **2**, e434 (2007).
- [33] C. Espinosa-Soto, O. C. Martin, and A. Wagner, *J Evol Biol* **24**, 1284 (2011).
- [34] M. Inoue and K. Kaneko, *PLoS Comput Biol* **9**, e1003001 (2013).
- [35] M. Inoue and K. Kaneko, *Eutophys Lett* **124**, 38002 (2018).
- [36] C. Furusawa and K. Kaneko, *PLoS Comput Biol* **4**, e3 (2008).
- [37] M. Pujato, T. MacCarthy, A. Fiser, and A. Bergman, *PLoS Comput Biol* **9**, e1002865 (2013).
- [38] J. J. Hopfield and D. W. Tank, *Biol Cybern* **52**, 141 (1985).
- [39] J. Lee, *Phys Rev Lett* **71**, 211–214 (1993).
- [40] F. Wang and D. P. Landau, *Phys Rev Lett* **86**, 2050– (2001).
- [41] F. Wang and D. P. Landau, *Phys Rev E* **64**, 056101 (2001).
- [42] J. J. Tyson, K. C. Chen, and B. Novak, *Curr Opin Cell Biol* **15**, 221 (2003).
- [43] M. Ptashne and A. Gann, *Genes & Signals* (Cold Spring Harbor Laboratory Press, 2002).
- [44] M. Ptashne, *A Genetic Switch (third edition)* (Cold Spring Harbor Laboratory Press, 2004).
- [45] C. Zong, L. h. So, L. A. Sepuveda, S. O. Skinner, and I. Golding, *Mol Syst Biol* **6**, 440 (2010).
- [46] J. D. Watson, T. A. Baker, S. P. Bell, A. Gann, M. Levine, and R. Losick, *Molecular Biology of the Gene (7th edition)* (Pearson Education, 2013).
- [47] J. E. Ferrell and E. M. Machleder, *Science* **280**, 895

- (1998).
- [48] S. Huang, Y.-P. Guo, G. May, and T. Enver, *Dev Biol* **305**, 695 (2007).
- [49] D. Jia, M. K. Jolly, W. Harrison, M. Boareto, E. Ben-Jacob, and H. Levine, *Phys Biol* **14**, 035007 (2017).
- [50] B. Huang, M. Lu, D. Jia, E. Ben-Jacob, H. Levine, and J. N. Onuchic, *PLoS Comput Biol* **13**, e1005456 (2017).
- [51] S. S. Shen-Orr, R. Milo, S. Mangan, and U. Alon, *Nat Genet* **31**, 64 (2002).
- [52] S. Mangan and U. Alon, *Proc Natl Acad Sci USA* **100**, 11980 (2003).
- [53] J. E. Ferrell and W. Xiong, *Chaos* **11**, 227 (2001).
- [54] J. E. Ferrell, *Curr Open Chem Biol* **6**, 140 (2002).
- [55] D. Angeli, J. E. Ferrell, and E. D. Sontag, *Proc Natl Acad Sci USA* **101**, 1822 (2003).
- [56] B. Pfeuty and K. Kaneko, *Phys Biol* **6**, 046013 (2009).
- [57] A. Tiwari and O. A. Igoshin, *Phys Biol* **9**, 055003 (2012).
- [58] J. E. Ferrell and S. H. Ha, *Trends Biochem Sci* **39**, 612 (2014).
- [59] C. Tan, P. Marguet, and L. You, *Nat Chem Biol* **5**, 842 (2009).
- [60] K. Sato, Y. Ito, T. Yomo, and K. Kaneko, *Proc Natl Acad Sci USA* **100**, 14086 (2003).